arXiv:1401.2779v2 [physics.ins-det] 11 Mar 2015

Simulation studies of hadron energy resolution as a function of iron plate thickness at INO-ICAL

S.M. Lakshmi,[1] A. Ghosh,[2] M. M. Devi,[3] D. Kaur,[4]
S. Choubey,[2] A. Dighe,[3] D. Indumathi,[1] M.V.N. Murthy[1] and Md. Naimuddin[4]

[1] *The Institute of Mathematical Sciences, Chennai 600 113, India*
[2] *Harishchandra Research Institute, Allahabad 211 002, India*
[3] *Tata Institute of Fundamental Research, Mumbai 400 005, India*
[4] *Department of Physics, Delhi University, New Delhi 110 007, India*

March 13, 2015

Abstract

We report on a detailed simulation study of the hadron energy resolution as a function of the thickness of the absorber plates for the proposed Iron Calorimeter (ICAL) detector at the India-based Neutrino Observatory (INO). We compare the hadron resolutions obtained with absorber thicknesses in the range 1.5–8 cm for neutrino interactions in the energy range 2–15 GeV, which is relevant to hadron production in atmospheric neutrino interactions. We find that at lower energies, the thickness dependence of energy resolution is steeper than at higher energies, however there is a thickness-independent contribution that dominates at the lower thicknesses discussed in this work. As a result, the gain in hadron energy resolution with decreasing plate thickness is marginal. We present the results in the form of fits to a function with energy-dependent exponent.

1 Introduction

The proposed India-based Neutrino Observatory (INO) is an underground laboratory designed primarily for the study of neutrinos from various sources.

One of the first and largest detectors at INO will be a magnetized iron calorimeter (ICAL) detector to primarily study atmospheric muon neutrinos (and anti-neutrinos). The ICAL detector is a calorimeter which comprises a stack of iron plates interleaved with Resistive Plate Chambers (RPC)[1, 2] as active detector elements.

Muons produced in the charged-current (CC) interactions of atmospheric muon (anti-)neutrinos with the iron target can be easily detected in ICAL. Their energy and momentum will be reconstructed using either the track length in the detector and/or the curvature due to the magnetic field. The magnetic field allows the charge identification as well.

The main difficulty in reconstructing the energy and direction of the incident neutrino arises from the uncertainty in energy and direction of the associated hadrons, mainly pions produced in interactions at neutrino energies of $\gtrsim 1$ GeV. Only hit multiplicity in the RPC layers and its distribution are available in the study of hadron response of ICAL [3]. Furthermore, the hits are restricted to a few layers only in contrast to the long track of the minimum ionising muons.

A potentially crucial factor in the determination of hadron energy and direction resolution is the thickness of the absorber material, i.e., iron. This must be optimised taking into account the physics goals of the experiment, apart from the detector size, geometry, stability and cost. In this simulation study, the effect of the variation in plate thickness on hadron energy resolution is analysed using fixed energy single pions. Earlier, such studies have concentrated on very high energy hadrons from tens of GeV to hundreds of GeV in hadron calorimeters [4, 5, 6, 7]. These studies have indicated a square root dependence on the thickness t of the hadron energy resolution on the absorber thickness. But no corresponding systematic analysis of the absorber thickness dependence at lower energies, in the GeV region, is found in the literature, although the values of the hadron energy resolution at some fixed thicknesses are available. Naively, hadrons traversing the plates at an angle θ will "encounter", in principle, an effective plate thickness $(t/\cos\theta)$ so that the thickness dependence can be explored through this angle dependence. However, in the actual detector, the detector geometry including support structures, and orientation as well as the arrangement of the detector elements introduce additional nontrivial dependence on thickness. This is what this work intends to understand.

The main focus of this report is to present the results of a simulation study of the thickness dependence of hadron energy resolution in the energy range 2–15 GeV. This energy domain is of primary importance to neutrino oscillations studies with ICAL. The default design of ICAL at present uses iron plates of thickness 5.6 cm. The energy resolution of hadrons (both for

fixed energy single pions as well as for multiple hadrons from CC interactions of neutrinos with iron) propagating in the default configuration of the ICAL detector has been discussed in Ref. [3]. Here, we study the effect of varying the plate thickness in the range of 1.5 to 8 cm.

The report is structured as follows. In Section 2, the detector configuration and the methodology of the analysis are outlined. The energy dependence of the hadron energy resolutions with different plate-thicknesses is discussed in Section 3. The results for the thickness dependence of the resolution parametrised in the form $p_0 t^{p_1} + p_2$ are presented in Section 4. Energy resolutions in different bins of $\cos\theta$, where θ is the incident hadron direction, and their thickness dependences are discussed in Section 5. Section 6 compares ICAL simulations with test beam data and simulations from both MONOLITH and MINOS. We conclude with a brief discussion and summary in Section 7.

2 Detector configuration and methodology

The default configuration of ICAL detector has three modules of 151 layers of 5.6 cm thick magnetized iron plates interleaved with RPCs; each module has a dimension of 16 m $\times$ 16 m $\times$ 14.45 m. The RPCs are placed in the 4 cm gap between two iron plates. Copper pickup strips of width 1.96 cm above and below each RPC, aligned transverse to each other, determine the x and y coordinates of the hit. The layer number gives the information about the z-coordinate. The x-, y- and z- axes are defined with respect to an origin located at the center of the detector, with the x axis along the largest dimension of the detector. For more details of the geometry and analysis, see Ref. [3].

A GEANT4-based [8] simulation framework has been used for the current analysis. The strip width and spacing between plates are kept unchanged while changing the plate thickness. In order to maintain the approximate weight of the detector for each plate thickness, the number of iron plates (and hence the number of RPC layers) are adjusted accordingly. This does not affect the analysis since the few GeV hadrons which this study focuses on traverse only a few layers and rarely reach the detector edges.

Pions, which constitute the major fraction of hadrons produced in neutrino interactions in the detector mainly propagate as showers. The hits in the shower are denoted as x-hits or y-hits depending on whether the information originated from the x- or the y-pickup strip. The maximum of these two numbers in a layer, named as orig-hits, is chosen for the study. As shown in our previous work [3], the analysis is not sensitive to this choice.

The study has been performed using fixed energy single positive pions (π^+). For obtaining the hit information, fixed energy single pions are propagated from random vertices inside a volume of 200 cm $\times$ 200 cm $\times$ 200 cm in the centre of the detector. This ensures that the event is completely contained inside the detector. The direction of propagation is determined by their zenith angle θ and the azimuthal angle ϕ in this geometry which is oriented such that the x-axis (the coordinate system is defined earlier) corresponds to $\phi = 0$ and the z-axis corresponds to the vertically up direction, with $\theta = 0$. Unless otherwise specified, θ is smeared from 0 to π and ϕ is smeared from 0 to 2π in order to obtain direction-averaged energy resolutions. The pion energy is varied from 2 GeV to 15 GeV in steps of 0.25 GeV without smearing. For each energy and plate thickness, we simulate 10000 events. Eleven plate thicknesses including the default value 5.6 cm are used. The thickness is varied from 1.5 cm in steps of 0.5 cm upto 5 cm and the other thicknesses are 5.6 cm, 6 cm and 8 cm.

As expected, the mean number of hits increases with decreasing plate thickness, and the width of the distribution also becomes broader. This is illustrated in Fig. 1 which shows the hit distributions for different iron plate thicknesses for a 5 GeV pion (π^+). It was found that the magnetic field did not change the hit distribution. This is due to the nature of shower development and multiple scattering effects in the case of hadrons.

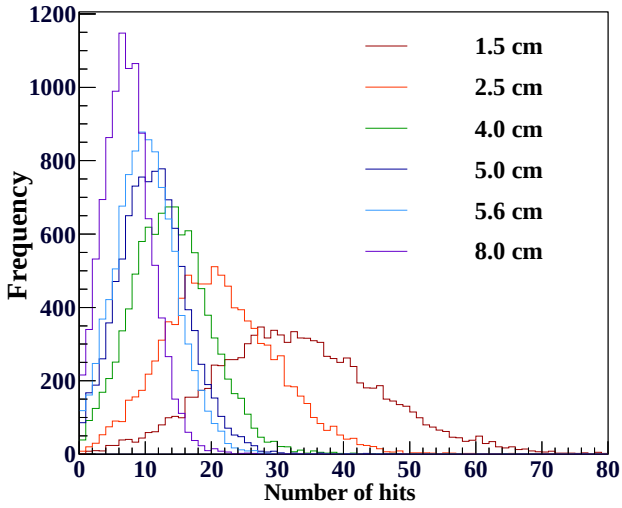

Figure 1: Hit distributions of 5 GeV single pions (π^+) propagated through sample iron plate thicknesses.

For the comparison of energy resolution at different thicknesses, we choose to use the mean and rms width (σ) of the hit distributions at different ener-

gies. We use σ/E as the indicator of energy resolution.

We parametrise the hadron energy resolution as $\sigma(E)/E = \sqrt{(a^2/E + b^2)}$, where $\sigma(E)$ is the width of the distribution, a is the stochastic coefficient which depends on the thickness of the absorber and b is a constant. The analysis is done by taking the square of the equation since it gives a linear relation between $(\sigma/E)^2$ and $1/E$ with a^2 as the slope and b^2 as the intercept:

$$\left(\frac{\sigma}{E}\right)^2 = \frac{a^2}{E} + b^2 \ . \tag{1}$$

Note that the parameters a and b are, in general, thickness dependent.

3 Energy resolution for different plate thicknesses

Energies of interest between 2–15 GeV are used in the analyses presented here. The arithmetic mean and rms width of the hit distributions in the energy range 2–15 GeV, for various thicknesses, are shown in Fig. 2.

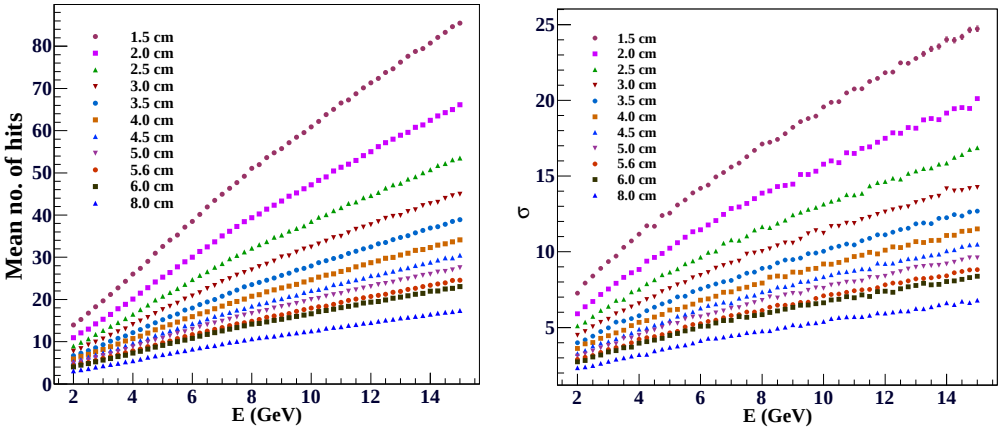

Figure 2: (Left) Mean number of hits and (Right) width of hit histograms as functions of pion energy E (GeV), in the energy range 2–15 GeV.

In the energy region below about 5 GeV, all processes including quasi-elastic (nucleon recoil), resonance and deep inelastic scattering can contribute to a comparable extent to the production of hadrons in neutrino interactions in the detector. In contrast, the high energy region is dominated by hadrons created via deep inelastic scattering. Keeping this distinction in mind, we

analyse the response to fixed energy single pions in two energy ranges, 2–4.75 GeV and 5–15 GeV, separately.

The ratio $\sigma/\text{Mean} = f(E,t)$ is identified as the resolution [3] and its square is fitted to the form given in Eq. (1), where t is the thickness of the absorber (iron plate) in cm (alternatively, it can be parametrised as t/t_0 where t_0 is a test or standard thickness; here $t_0 = 1$ cm).

One has to determine the specific functional form of the thickness dependence of the parameters a and b on the right hand side of Eq. (1). Before doing this, it is important to determine the values of a and b for different thicknesses by fitting this form in the two different energy ranges as specified earlier.

3.1 Energy range 2–4.75 GeV

We first analyze the low energy region which is the most relevant for atmospheric neutrino studies with the ICAL detector. The square of the resolution, $(\sigma/\text{Mean})^2$, for the thicknesses from 1.5–8.0 cm, plotted as a function of $1/E$, where E is the pion energy in GeV, is shown in Fig. 3. It can be seen that a increases significantly with thickness as evinced by the increase in slope ($= a^2$) of the fit with thickness, with a increasing from $a = 0.65$ to $a = 0.97$ as the thickness increases. However, b, as determined by the intercept ($= b^2$), is nearly constant in comparison, as it ranges from $b = 0.28$ to $b = 0.31$ with increase in thickness.

3.2 Energy range 5–15 GeV

We study the higher energy region separately to probe a possible stronger E-dependence. Fig. 3 shows that the behaviour is similar to the low energy case. Typically, the value of the stochastic coefficient a varies from 0.70–0.97, which is higher than in the lower energy case by up to 10%, whereas b varies from about 0.23–0.30.

Having determined the stochastic and constant parameters in these different energy ranges for different thicknesses, we now proceed to study the thickness dependence of the hadron energy resolutions.

4 Parametrisation of the plate thickness dependence

The functional form of the thickness dependence is introduced in two different ways. In the first approach, the thickness dependence is attributed entirely

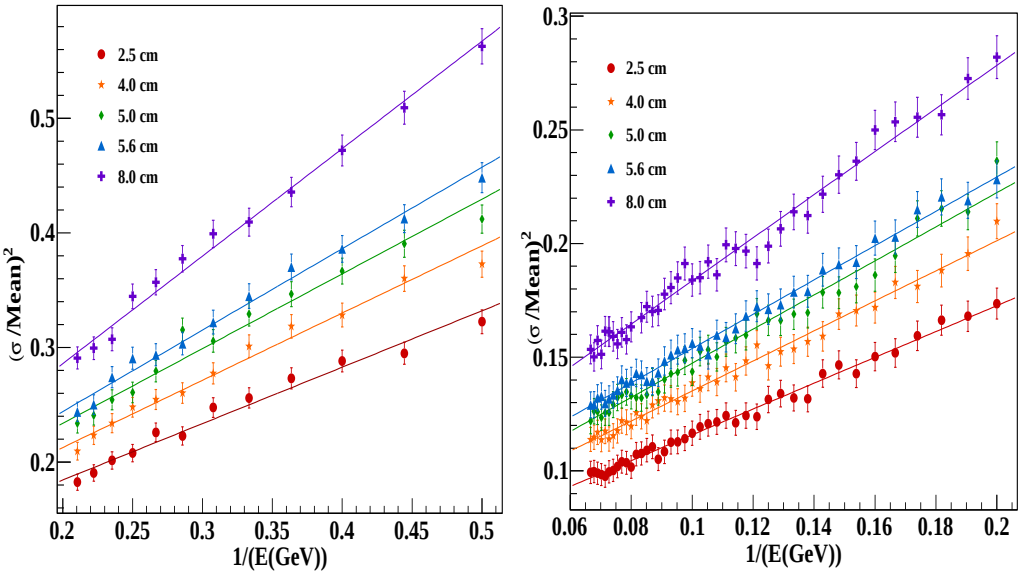

Figure 3: Plots of $(\sigma/\text{Mean})^2$ versus $(1/E(\text{GeV}))$ fitted to Eq. (1) in the energy range 2–4.75 GeV (left panel) and 5–15 GeV (right panel). The thickness varies from 2.5 cm to 8 cm from bottom to top.

to the stochastic coefficient, a. This is motivated by the observation that the parameter b has a much smaller dependence on the thickness, as can be seen from the analyses above. The thickness dependence of the stochastic coefficient a is parametrised in the standard form,

$$a(t) = p_0 t^{p_1} + p_2 \ , \tag{2}$$

where p_2 is the limiting resolution for hadrons for finite energy in the limit of very small thickness due to the nature of their interactions, detector geometry and other systematic effects. We estimate these parameters in suitably chosen energy ranges as mentioned before.

We use Eq. (2) to determine the thickness dependence of the stochastic coefficient a separately in three different energy ranges as mentioned earlier. The parameters p_i $(i = 0, 1, 2)$ are determined independently in each energy range.

In Fig. 4, we show the fits in the energy ranges 2–4.75 GeV and 5–15 GeV as functions of thickness. The parameters p_0, p_1, and p_2 obtained from the fit to the form given in Eq. (2) are also shown in the figure. The thickness dependence is given by the exponent p_1. From the fit value shown in Fig. 4, p_1 is clearly energy-sensitive and decreases in the higher energy range.

The analyses followed in the two energy ranges show that the dependence on the thickness is stronger than $\sqrt{t}$; however, note the smallness of p_0, the

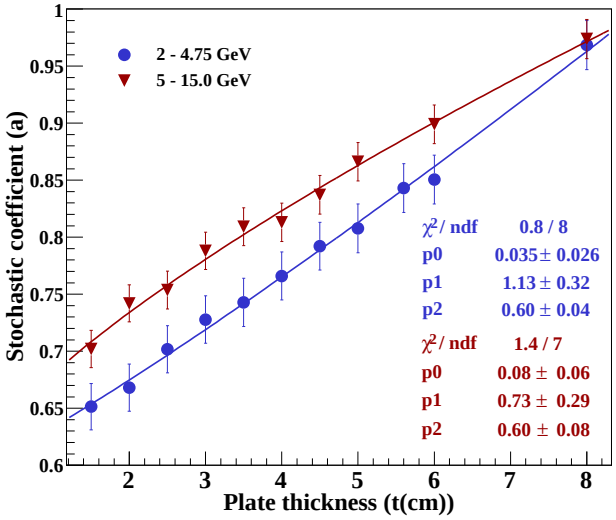

Figure 4: The stochastic coefficient a obtained from the analysis in the energy ranges 2–4.75 GeV and 5–15 GeV versus the plate thickness t in cm, fitted with Eq. (2).

coefficient of the thickness parameter, in all cases, in comparison with the constant parameter p_2. Irrespective of the energy range, it remains around $p_2 \sim 0.60 \pm 0.08$ and contributes substantially to the resolution. This means that *there will always be a residual resolution which cannot be improved further by reducing the thickness*, thereby making the option of going to smaller thicknesses less attractive than what the bare t-dependence indicates. For example, although the resolution has an approximately linear dependence on the thickness ($p_1 \sim 1.1$) at low energy, it worsens by only about 15% when the thickness doubles from $t = 2.5$ to $t = 5$ cm rather than doubling as the bare t dependence indicates.

An alternative approach is to analyse the thickness dependence of the entire width and not just that of the stochastic coefficient. The analysis was done for different energies. A fit to $\sigma/\sqrt{E}$ with the equation

$$\sigma/\sqrt{E} = q_0 t^{q_1} + q_2 \ , \tag{3}$$

congruent in form with Eq. (2), reveals the following trend as illustrated in Fig. 5. The exponent q_1 of the absorber thickness (t(cm)) decreases from $\sim$ 0.9 to 0.66 in the 2–15 GeV energy range, whereas its coefficient q_0 increases from $\sim$ 0.06–0.14 with energy. The constant term q_2 increases from $\sim$ 0.65–0.98 with energy E (GeV). Again, the smallness of the coefficient q_0 results in the q_2 dominating over the term $q_0 t^{q_1}$. Thus the behaviour closely parallels that of the earlier analysis with the thickness dependence of a alone. We

also show linear fits for the E dependence of the parameters q_0, q_1 and q_2 in Fig 5. The trends indicate that the thickness exponent mildly decreases with energy and may therefore be compatible with the square-root results of earlier studies at higher beam energies [4, 9].

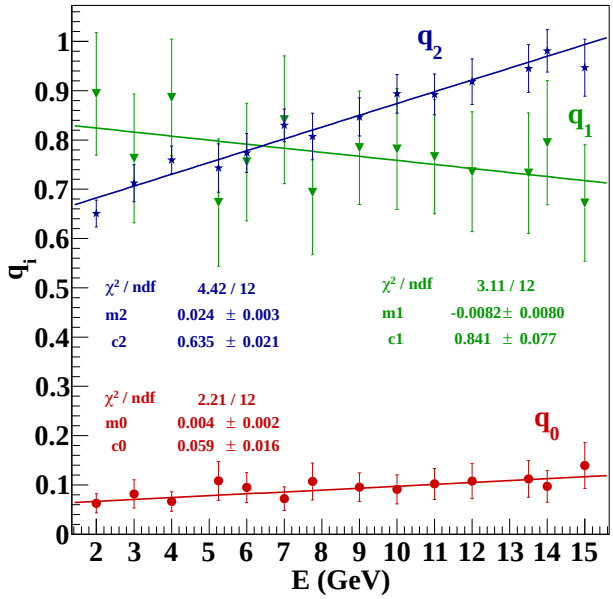

Figure 5: Variation of the parameters q_i obtained by fitting $\sigma/\sqrt{E}$ to Eq. (3) in the energy range 2–15 GeV. The linear fits through the points indicate the E dependence for each parameter.

We have focussed here on single pions since we are interested in understanding the thickness dependence. However, ICAL will be built to study charged-current neutrino interactions where multiple hadrons may be produced in the final state, from either resonance or deep inelastic interactions. A brief remark about hadrons from neutrino interactions is therefore in order. The study of such final states where the hadronic energy is shared by more than one hadron will bring additional uncertainty in the study of thickness dependence.

An earlier study [3] for a fixed absorber thickness of $t = 5.6$ cm compared single pion resolutions with those of events generated by the NUANCE neutrino generator [10] where multiple hadrons are produced in the final state and there is a non-trivial partition of energy into the different hadronic final states. The trends in the dependence of the resolution (quantified by σ/E as well as the stochastic coefficient a) were found to be similar in the single-pion and multi-hadron cases. This can be understood from the e/h response of ICAL; details are given in Appendix A. Again, we find that the thickness

dependence from the NUANCE data sample has a similar behaviour to the single pion case.

The effect of different hadron models on resolutions were also studied by replacing the LHEP model that was used in GEANT4 [8] with QGSP (for 12 GeV hadrons) and QGSP_BERT (for the lower energy hadrons). The resolution was found to be reasonably model independent, with a variation in the mean (rms) of less than 4% (5%) among different models in the energy range from 2–15 GeV for $t = 5.6$ cm.

5 Angular dependence of energy resolution and thickness dependence

So far, we have considered hadrons smeared in all directions in both polar and azimuthal angles, θ and ϕ. In this section we present the energy resolution in various bins of incident polar angle θ. The azimuthal angle ϕ is still smeared from 0–2π in each θ bin. The bins are defined symmetrically over the up/down directions in intervals of 0.2 in $|\cos\theta|$, with the averages corresponding to $\langle|\cos\theta_{in}|\rangle = 0.9$, 0.7, 0.5, 0.3 and 0.1 respectively. The bins with the largest $|\cos\theta|$ are nearly perpendicular to the iron plates (and we refer to them as vertical events) while the ones with the smallest values are practically parallel to them (and we label them as horizontal events). As an example, the energy resolution for a 5 GeV pion in different angular bins as a function of plate thickness (t (cm)) is shown in Fig. 6.

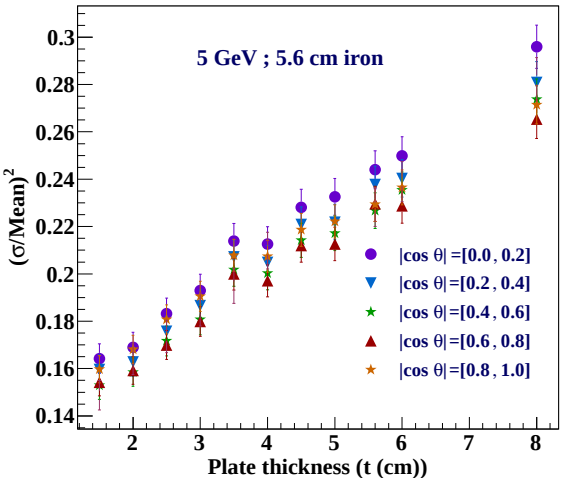

Figure 6: Energy response of a 5 GeV pion as a function of various thicknesses in different incident $\cos\theta$ bins.

Several observations are in order. Firstly, hadrons in the horizontal bin have the worst resolution, as expected. The resolution generically improves with increasing $|\cos\theta|$, except in the vertical bin ($|\cos\theta| = 0.8$–1.0) for all thicknesses. This is due to the geometry of the detector, with support structures at every 2 m in both the x- and y-directions. This reduces the region of sensitive detector in the vertical direction, with a consequent loss of resolution. Finally, while the hadron traverses an effective thickness of $t/\cos\theta$, the resolution does not exhibit such a naive scaling behaviour. It is seen that, for the same value of $t/\cos\theta$, the resolution is better at smaller thicknesses than at larger thicknesses. This is again because of the non-trivial geometry and other factors.

A similar trend is seen at all energies; the energy resolution in each $\cos\theta$ bin, in the energy range 5–15 GeV, is shown in Fig. 7 for the default thickness of $t = 5.6$ cm. The thickness dependence in the angular bins is shown most conveniently in terms of the stochastic coefficient a as determined from fits in the energy range 5–15 GeV and has also been plotted in Fig. 7.

Since there is only a mild dependence on the hadron direction, the direction-averaged results obtained in the earlier sections present a realistic picture of the thickness dependence of the energy resolution of hadrons.

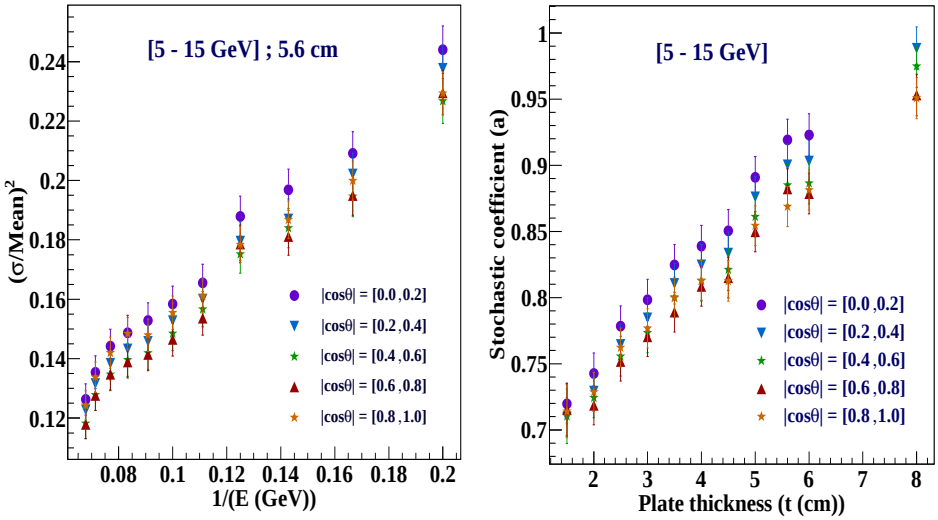

Figure 7: (Left) Energy resolution in bins of incident θ in the energy range 5–15 GeV for the default iron thickness of $t = 5.6$ cm. (Right) Stochastic term a vs plate thickness in various incident θ bins for the energy range 5–15 GeV.

6 Comparison with other experiments

For the validation of the analysis presented here, the result of ICAL simulation has been compared with both simulations of MONOLITH and MINOS collaborations and also to the data from the test beam runs conducted by them. In the current simulation, ICAL with 8 cm iron plate has a resolution of $98.5\%/\sqrt{E} \oplus 29.4\%$ which is roughly comparable to the angle-averaged result of $90\%/\sqrt{E} \oplus 30\%$ obtained from the simulation studies of MONOLITH [11] with the same plate thickness. For convenience of comparison, the convention $a/\sqrt{E} \oplus b \equiv \sqrt{a^2/E + b^2}$ has been used.

Our results cannot be directly compared with the test beam data since beams are highly directional (with $\cos\theta = 1$ as the beam divergence is typically small). To enable a comparison with the beam data we consider events where the hadrons are normally incident on the detector plates.

MONOLITH has performed a test beam run with 5 cm iron plates (Baby MONOLITH) with the T7-PS beam at CERN [12, 13]. This beam provides pions of energies ranging from 2–10 GeV which are exactly normally incident on the iron plates. The run reported an energy resolution of $68\%/\sqrt{E} \pm 2\%$. The simulation of ICAL detector with 5 cm iron plates with single pions of energies 2–10 GeV incident normally on the detector at a fixed vertex $(100, 100, 0)$ cm, is shown in Fig. 8. The analysis gives a similar energy resolution of $66.3\%/\sqrt{E} \oplus 8.7\%$.

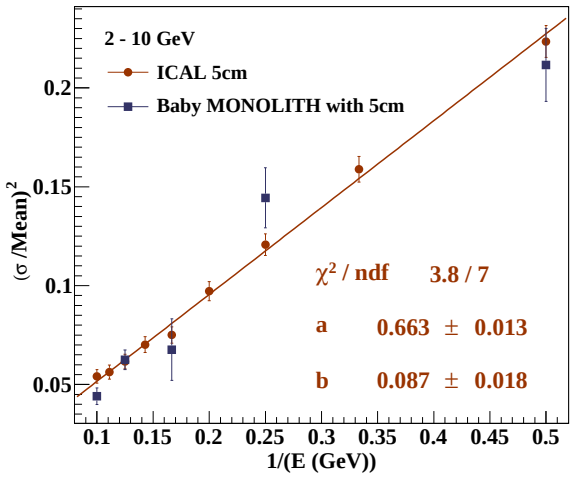

Figure 8: Energy response of ICAL detector with 5 cm thick iron plates with single pions in the energy range 2–10 GeV, propagated from the vertex fixed at $(100, 100, 0)$ cm in the vertical direction, compared with the data from MONOLITH test beam run [12, 13].

The simulation studies with gaseous detectors by MINOS collaboration have reported a hadron energy resolution of $70\%/\sqrt{E}$ with $1.5''$ (i.e., 3.8 cm) iron plates [14]. The test beam run of MINOS with APT (Aluminium Proportional Tubes) active detectors and $1.5''$ steel plates in the energy range 2.5–30 GeV was reported to have a hadron energy resolution of $71\%/\sqrt{E}\oplus 6\%$ [9]. ICAL simulation with 4 cm iron plates in the energy range 2–30 GeV gives a resolution of $61\%/\sqrt{E}\oplus 14\%$. The results are compatible, considering that there are differences in detector geometries.

Our simulation results thus agree with those of MINOS and MONOLITH simulations and test beam results within statistical errors. The slight differences can be attributed to differences in the details of the detector configuration. Note also that fixed vertex data tend to give smaller values of b than the smeared vertex case; this is because the hadrons see more inhomogeneities in the detector geometry in the latter case, and this is reflected in the larger residual resolution.

7 Conclusions

We have made a simulation study of the direction-averaged hadron energy resolution as a function of iron plate thickness (from 1.5 to 8 cm) in the energy range of interest for atmospheric neutrino interactions. The study was motivated by the realisation that the hadron energy resolution is a crucial limiting factor in reconstructing the neutrino energy in charged current interactions of atmospheric neutrinos in the magnetized Iron CALorimeter (ICAL) detector at the proposed India-based Neutrino Observatory (INO). The analysis was done by propagating pions in the simulated ICAL detector at various fixed energies, averaged over all directions (θ, ϕ) in each case.

Simulations show that the hadron energy resolution depends on plate thickness t (cm) through a relation $a = p_0\, t^{p_1} + p_2$, where a, the stochastic coefficient, is the energy-dependent term in the standard resolution, $(\sigma/E)^2 = a^2/E + b^2$. That is, there is a finite energy resolution for hadrons even when the plate thickness is small. This reflects the strong nature of hadronic interactions with matter (iron in this case) that leads to large systematic uncertainties. We find that the constant term p_2 is always dominant compared to the first t-dependent term because the coefficient p_0 of the t^{p_1} term is small; hence reducing the plate thickness does not lead to a significant gain in the hadron energy resolution. This is true over all the thicknesses studied in the energy range 2–15 GeV.

Similar results are obtained when the quantity $\sigma/\sqrt{E} = q_0 t^{q_1} + q_2$ is studied for its thickness dependence. The trends of the fit parameters q_i

as functions of E (GeV) show that the the smallness of the coefficient q_0 is again responsible for the dominance of the thickness independent term q_2. The results were also reasonably insensitive to the choice of hadron model within GEANT.

The energy resolution was also studied as a function of the incident angle θ for different thicknesses t. It was found that the thickness dependence of the resolution did not satisfy the naive expectation of being proportional to $t/\cos\theta$; this is because of the detector geometry with the distribution of its sensitive elements also playing a role. On the whole, the angular dependence is not strong. While the resolution did improve with increasing $|\cos\theta|$ as expected, the vertical hadrons were not as well-resolved as would have been the naive expectation because of the presence of dead spaces such as detector support structures, etc.

Comparisons of ICAL simulations with those of MONOLITH and MINOS and their test beam runs have been conducted and are found to match.

The final choice of the plate thickness will depend not only on the behaviour of hadrons but also on on the energy range of interest to the physics goals of the experiment. Issues like low energy muons, the threshold energy, possibility of electron detection, cost etc will also affect the choice of plate thickness. But these are outside the scope of this simulation study.

Acknowledgement

We thank G. Majumder, A. Redij for the development of the simulations framework for ICAL; B. Choudhary, V.M. Datar and Y.P. Viyogi for the critical comments and suggestions on the manuscript and content. We also thank N.K. Mondal, P. K Behera and all members of the INO collaboration who gave their comments and suggestions in the weekly simulations meetings. We thank the Department of Atomic Energy (DAE), India, and Department of Science and Technology (DST), India, for supporting this research work.

Appendix A: Study of e/h ratio in the context of plate thickness dependence

A hadron shower consists of both hadronic and electromagnetic parts. The electromagnetic part of a hadron shower originates from the neutral pions π^0. The response of neutral pions is similar to that of electrons since the π^0 decays almost immediately into electron-positron pairs. Hence a study of the

ratio of electron response to charged pion response, i.e, the e/h ratio, helps us characterise the effect of neutral hadrons on the energy resolution.

We have conducted the simulation studies of the e/h ratio in ICAL detector using fixed energy single electrons and pions. Here, 1,00,000 single particles, this time electrons, are generated in the energy range 2–15 GeV and are propagated in arbitrary directions (with θ smeared from $0 - \pi$ and ϕ from $0 - 2\pi$) within a volume of 2 m $\times$ 2 m $\times$ 2 m in the central region of the ICAL detector for different iron plate thicknesses. The response is very smooth as a function of thickness; hence the results only for 5.6 cm and 2.5 cm are shown in Fig. 9. The hit distributions averaged over all directions for $2, 5, 10$ and 14 GeV electrons in the two sample iron plate thicknesses 2.5 cm and 5.6 cm are illustrated in Fig. 9. For reference, the corresponding pion hit distributions at 5 GeV have been illustrated in Fig. 1.

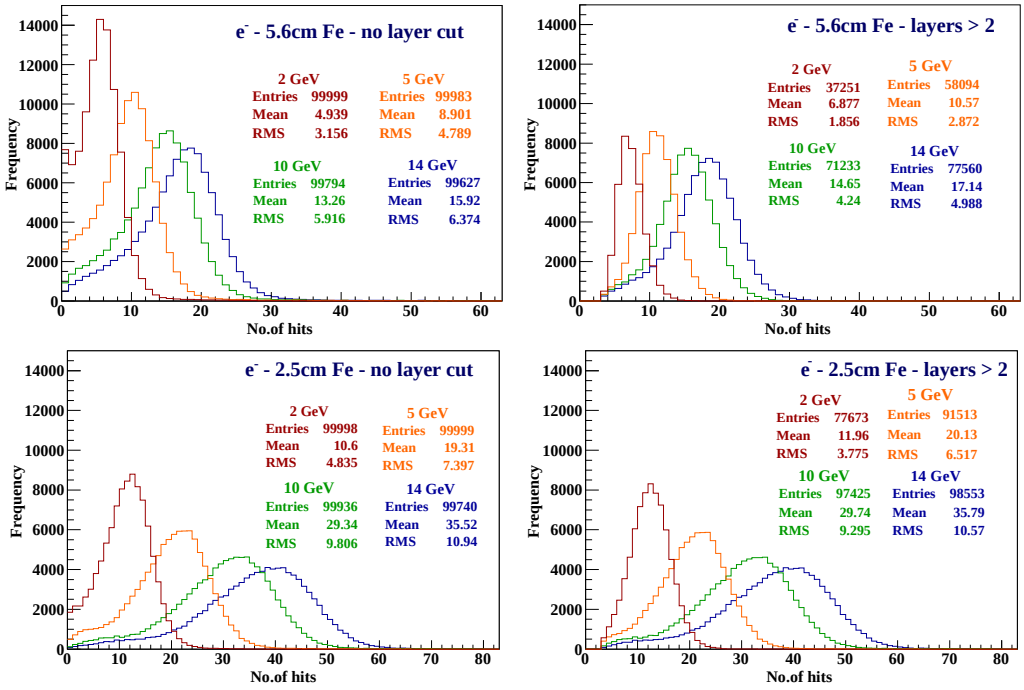

Figure 9: Hit distributions of fixed energy single electrons at 2, 5, 10 and 14 GeV in 5.6 cm (top) and 2.5 cm (bottom) thick iron, averaged over all directions. The left panels show the distributions without any layer cut and the right panels those with the layer cut of $l > 2$, where l is the number of layers containing hits.

It can be seen that the peak positions are not very different between electrons and pions; however, there are many more zero hits in the former

especially at the higher thickness of 5.6 cm due to the large energy loss of electrons in the iron. This can be improved by imposing a selection criterion that hits must be present in at least 3 layers in each event. As can be seen in the right hand panels of Fig. 9, the histograms are then more symmetrical about the peak, which is now shifted to the right. In addition, this criterion primarily affects results at higher thicknesses and lower energies, where the layer cut improves the hit distribution significantly although the reconstruction efficiency is reduced. As the thickness reduces, the layer cut does not affect the hit distribution significantly, except at low energies below about 5 GeV.

The electron energy is calibrated to the mean number of hits as in the case of fixed energy single pions. The ratio of the electron response to charged pion response, i.e., the e/h ratio, is obtained as:

$$e/h = e^{-}_{mean}/\pi^{+}_{mean}, \tag{4}$$

where e^{-}_{mean} is the arithmetic mean of the electron hit distribution and π^{+}_{mean} is the arithmetic mean of the hit distribution for π^{+}. If $e/h = 1$, then the detector is said to be compensating. The variation of the e/h ratio with incident energy for the two sample thicknesses 2.5 cm and 5.6 cm are shown in Fig 10.

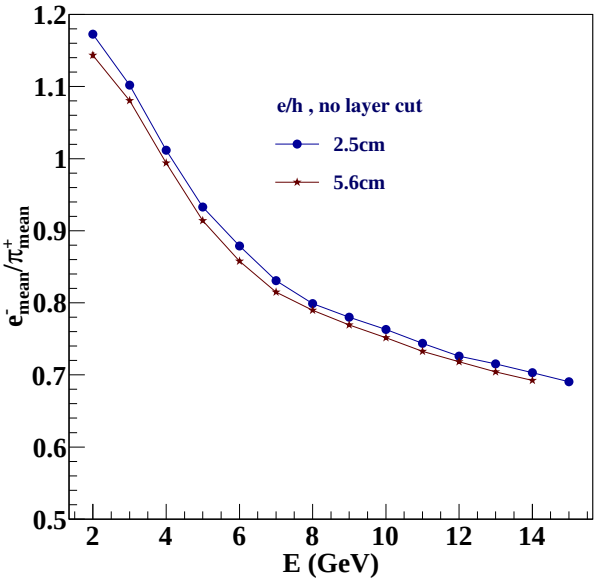

Figure 10: Variation of e/h ratio with incident energy for two different thicknesses namely 2.5 cm and 5.6 cm without any layer cut. It can be seen that the e/h ratio decreases with increase in energy.

It can be seen that the value of e/h decreases with energy. However, it should be noted that there is no direct measurement of the energy deposited in ICAL. Here the energy of a shower is simply *calibrated* to the number of hits, and electrons which travel smaller distances in a high Z material like iron have lower number of hits compared to charged pions. At lower energies the electron shower hits are concentrated around a small region. At these energies, the charged pions also do not traverse many layers in the detector due to the larger hadronic interaction length. This causes the mean of the electron hit distribution to be roughly the same or slightly larger than that of the π^+ hit distribution. But with the increase in energy, the charged pions travel more distance and hence give more hits (as they traverse more layers) since the hadronic interaction length is much more than the electromagnetic interaction length at higher energies and hence the ratio of hits in the two cases drops with energy. The layer cut only affects the low energy result by marginally decreasing the e/h ratio at $E < 4$ GeV, that too only for higher thicknesses.

In a neutrino interaction where all types of hadrons can be produced (although the dominant hadrons in the jet are pions), the response of ICAL to hadrons produced in the interaction depends on the relative fractions of charged and neutral pions. The NUANCE neutrino generator was used to generate charged current atmospheric muon neutrino events for the default ICAL thickness of 5.6cm. The fraction of the different types of hadrons obtained from a 100 year sample was found to be $\pi^+ : \pi^- : \pi^0 :: 0.38 : 0.25 : 0.34$, with the remaining 3% contribution mainly from kaons.

The average response of hadrons obtained from the charged current muon neutrino interaction can be expressed as:

$$\begin{aligned} R_{had} &= [(1 - F_0) \times h + F_0 \times e], \\ &= h\left[(1 - F_0) + F_0 \times \frac{e}{h}\right], \end{aligned} \tag{5}$$

where e is the electron response, h the charged hadron response and F_0 is the neutral pion fraction in the sample.

The atmospheric neutrino events of interest in ICAL are dominated by low energy events with hadrons typically having energies $E < 10$ GeV for which the average value of e/h is $e/h \approx 0.9$. Using $F_0 = 0.34$ in Eq. (6), we get the average hadron response for NUANCE-generated events to be $R_{had} = 0.97h$ which is not very different from h. For this reason, the analysis of response with multiple hadrons in NUANCE-generated events sample was not very different from that of the single pions sample, as discussed in Ref. [3].

References

[1] S. Athar *et al.*, India-based Neutrino Observatory Report, `http://www.ino.tifr.res.in/ino/OpenReports/INOReport.pdf`, May 2006.

[2] V.M. Datar *et al.*, Nucl. Instrum. Methods **A 602** (2009) 744–748.

[3] M.M. Devi *et al.*, *Hadron energy response of the Iron Calorimeter detector at the India-based Neutrino Observatory*, JINST **8** P11003, 2013, arXiv:1304.5115 [hep-ex].

[4] D. Green, *Physics of Particle Detectors*, Cambridge Monographs on Particle Physics, Nuclear Physics and Cosmology, (Cambridge University Press, 2000).

[5] D. Green, *Hadron Calorimeter Performance with a $PbWO_4$ EM Compartment*, FNAL TM-1958, Dec. 1995; lss.fnal.gov/archive/test-tm/1000/fermilab-tm-1958.pdf .

[6] C.W. Fabjan, *Calorimetry in high energy physics* CERN-EP/85-54, 1985.

[7] K. Kleinknecht, Phys. Rep. **84**, (1982) 85–161.

[8] S. Agostinelli *et al.*, *Geant4 - a simulation toolkit*, Nucl. Instrum. Methods **A 506** (2003) 250-303; `http://geant4.cern.ch/`.

[9] P. Schoessow *et.al.*, *Results from an iron-proportional tube calorimeter prototype*, NUMI-Note , MINOS Document 335-v1

[10] D. Casper, *The Nuance neutrino physics simulation, and the future*, Nucl. Phys. Proc. Suppl. **112** (2002) 161, [hep-ph/0208030].

[11] N.Y. Agafonova *et al.*, *MONOLITH: A massive magnetised iron detector for neutrino oscillation studies*, Monolith Proposal, LNGS P26/2000 CERN/SPSC 2000-031, SPSC/M657, 2000.

[12] M. Ambrosio *et al.*, *The MONOLITH prototype*, Nucl. Instrum. Methods **A 456** (2000) 67–72.

[13] G. Baria *et al.*, Nucl. Instrum. Methods **A 508** (2003) 170–174.

[14] D.A. Petyt, *A study of parameter measurement in a long-baseline neutrino oscillation experiment*, PhD thesis, University of Oxford, preprint FERMILAB-THESIS-1998-66 (1998), `www.physics.ox.ac.uk/neutrino/Petyt/Petyt.htm`.

[15] D. Green, *Calibration of the CMS Calorimeters*, 2001

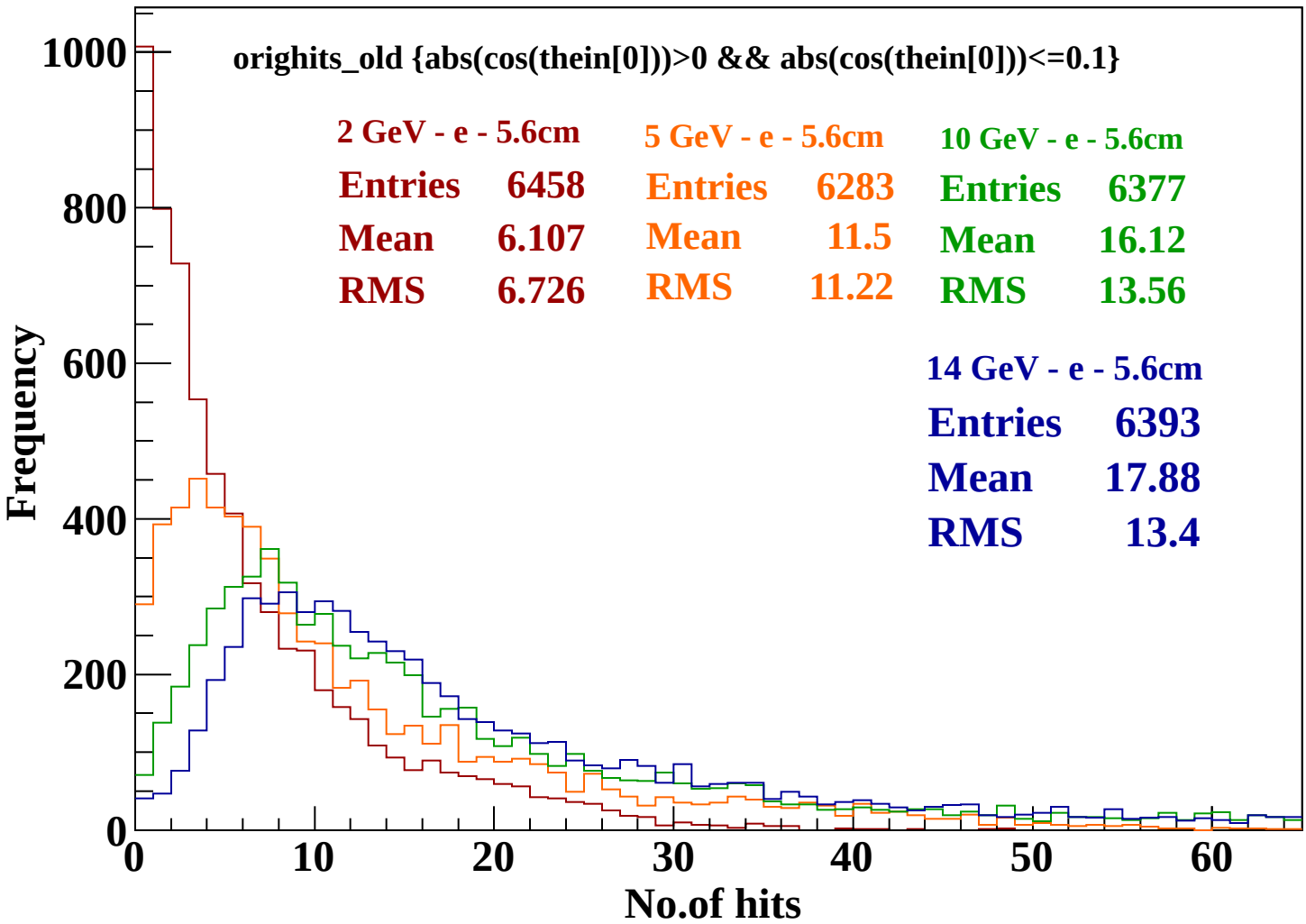
orighits_old {abs(cos(thein[0]))>0 && abs(cos(thein[0]))<=0.1}
2 GeV - e - 5.6cm
Entries 6458
Mean 6.107
RMS 6.726
5 GeV - e - 5.6cm
Entries 6283
Mean 11.5
RMS 11.22
10 GeV - e - 5.6cm
Entries 6377
Mean 16.12
RMS 13.56
14 GeV - e - 5.6cm
Entries 6393
Mean 17.88
RMS 13.4
Frequency
No.of hits
0
200
400
600
800
1000
0
10
20
30
40
50
60

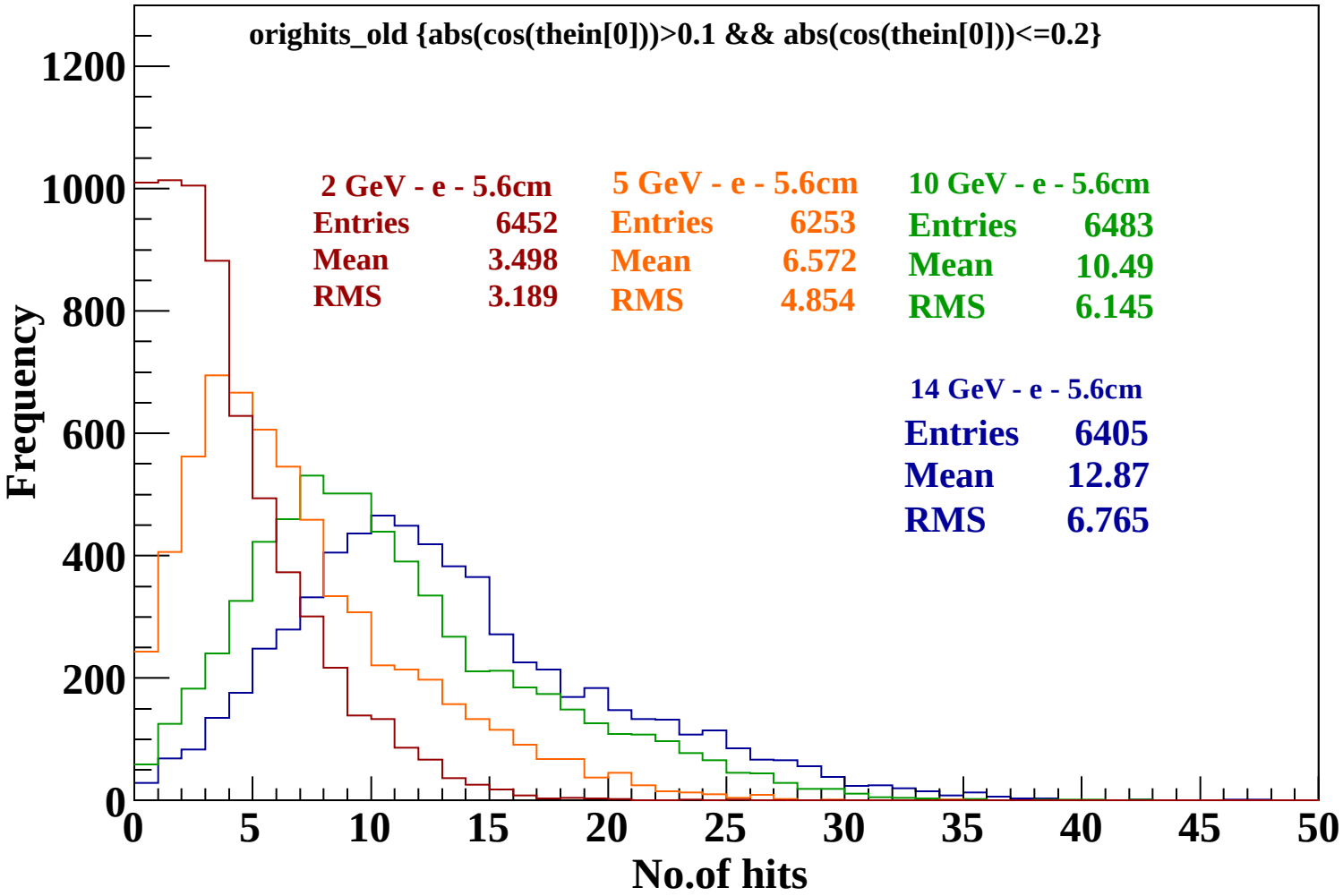
orighits_old {abs(cos(thein[0]))>0.1 && abs(cos(thein[0]))<=0.2}
2 GeV - e - 5.6cm
Entries 6452
Mean 3.498
RMS 3.189
5 GeV - e - 5.6cm
Entries 6253
Mean 6.572
RMS 4.854
10 GeV - e - 5.6cm
Entries 6483
Mean 10.49
RMS 6.145
14 GeV - e - 5.6cm
Entries 6405
Mean 12.87
RMS 6.765
Frequency
No.of hits
0
200
400
600
800
1000
1200
0
5
10
15
20
25
30
35
40
45
50